THESIS

ROLES OF RESIDUE MANAGEMENT, MICROBES AND AGGREGATION IN SOIL CARBON STABILIZATION UNDER SEMIARID, IRRIGATED CORN

Submitted by

Hanna Oleszak

Department of Soil and Crop Sciences

In partial fulfillment of the requirements

For the Degree of Master of Science

Colorado State University

Fort Collins, Colorado

Summer 2021

Master's Committee:

Advisor: M. Francesca Cotrufo
Co-Advisor: Catherine Stewart

Pankaj Trivedi

ABSTRACT

ROLES OF RESIDUE MANAGEMENT, MICROBES AND AGGREGATION IN SOIL CARBON STABILIZATION UNDER SEMIARID, IRRIGATED CORNFIELD

With atmospheric carbon dioxide levels continuously on the rise, it is critical that we focus our efforts on sequestering carbon (C) to slow global warming. To maximize these efforts, it is furthermore important to understand the pathways by which plant C inputs form soil organic carbon (SOC), as these pathways may inform the efficiency and duration of C stabilization. No-tillage is often recommended as a universal tool to draw C into the soil, yet literature reports mixed effects of tillage practices on C accrual. To maximize our efforts and best recommend agricultural practices for C sequestration, it is important to understand how the incorporation of residue within the mineral soil and disturbance associated with tillage impact plant residue C dynamics, as mediated by changes in microbial community and soil structure. While microbes play the active role in decomposing organic matter, soil structure can act as a gatekeeper to microbial accessibility to organic matter; thus, the effects of disturbance and residue incorporation upon the interplay of these two variables is highly important to consider. We used ^{13}C labeled plant residue to track the movement of residue C in incorporated vs. surface-applied residue treatments in irrigated, semiarid corn for a period of 30 months. Both carbon dioxide (CO_2) fluxes and soil cores were tested for total C and ^{13}C enrichment to quantify residue-derived C contribution to CO_2 efflux and to C accrual in the mineral soil over time, respectively. Furthermore, aggregate size fractionation and microbial community (via phospholipid fatty acids, PLFAs) were analyzed to assess how residue placement location and disturbance affect the

mechanisms behind residue decomposition, and ultimately soil C stabilization. The incorporation of residue in the mineral soil resulted in significantly greater SOC formation efficiencies and greater SOC accrual in the first year, compared to the surface-application of residue. However, differences in SOC accrual subsided after 30 months, even though higher CO_2 losses were measured in the surface applied residue treatments after 30 months. Residue-derived microbial biomass was greater in INC than SA or SA-NR at all timepoints, although this was only significant at 6 and 12 months. Residue-derived microbial community composition differed between early and later stages of decomposition, as well as between disturbed and undisturbed treatments. Mean weight diameters of aggregates featured a seasonal trend, with greater mean weight diameters in the fall. Furthermore, INC had significantly higher MWD at 5-10 cm at 6 months compared to surface-applied treatments, while disturbed treatments (INC and SA-NR) had significantly higher MWD's at depth at 12 months than SA. MWD was strongly correlated to residue-derived SOC in incorporated treatments, but not in surface-applied treatments. Finally, SOC formation efficiencies were more strongly correlated to residue-derived F:B in the incorporated treatment, compared to surface-applied treatments. Residue C recovery, SOC formation efficiencies, and residue-derived microbial biomass indicate that the incorporation of residue stimulates SOC formation through the DOC-microbial pathway and the physical transfer path concurrently, while the surface-application of residue follows a shift in SOC formation pathways from DOM-microbial SOC formation to physical transfer of residue. Additionally, correlations between residue-derived SOC, residue-derived F:B, and MWD indicate that the protection of residue C largely relies on aggregation when residue is incorporated.

ACKNOWLEDGEMENTS

My thesis would not have been made possible without the help of countless of collaborators. Firstly, I'd like to thank my advisors, Francesca and Cathy, for their expertise and guidance throughout these last two crazy years. I'd also like to thank Pankaj, my committee member and professor, for his insight, enthusiasm, and kindness. Finally, I thank everyone who contributed their time, energy, and knowledge to my project, particularly Liz Pruessner, Stuart Watts, Dan Reuss, Miho Yoshioka, Erin Grogan, Brad Floyd, John Frame, and the Cotrufo lab group.

Most importantly, I'd like to thank my Mom, Dad, and Luka, for their constant love, support, and encouragement; my brothers and Hillary, for the occasional laugh and change in perspective; my roommates, for their solidarity and good cooking; and most of all, my kotek Meeko, for sticking through the pandemic and my last semester of graduate school with me.

TABLE OF CONTENTS

CHAPTER 1: INTRODUCTION

An estimated 133 Pg of soil carbon (C) has been lost through the agricultural cultivation of undisturbed land (Sanderman et al., 2017), resulting in reduced soil quality and productivity (Lal et al., 2015). Therefore, there is significant potential to replenish soil C by utilizing conservation agricultural management practices, which also promote agricultural productivity, food security, and global warming mitigation (Stockmann et al., 2013; Paustian et al., 2016; IPCC, 2019). Accordingly, agricultural producers are increasingly turning towards the conservation practice of no-till (NT) management (USDA, 2020), which can result in greater C accrual than traditional, more intensive conventional tillage (CT) (Havlin et al., 1990; Paustian et al., 1997; Smith et al., 1998; Bayer et al., 2006). However, the relationship between tillage and soil C storage is not simple. Many studies have demonstrated no differences in total soil C accrual between tillage practices, but rather a redistribution of C between surface and at depth, with NT having an accrual of surface C and CT having C redistributed throughout the plow layer (Angers et al., 1997; VandenBygaart et al., 2003; Baker et al., 2007; Blanco-Canqui & Lal, 2008). Residue placement on the surface may allow additional C loss compared to residue that is physically mixed into, and potentially protected within, the soil (Manley et al., 2005, Mitchell et al., 2018; Leichty et al., 2020). To better understand these varied results, it is critical to elucidate the specific mechanisms by which the placement of residue affects soil organic C (SOC) formation and stabilization.

The transformation of C from plant-derived residue to SOC is largely mediated by soil microbes and their ability to access residue C substrates. During this process, residue C is either assimilated into microbial biomass, lost to the atmosphere as CO_2, released to the soil as

dissolved organic C (DOC), or protected from further decomposition by soil aggregation; residue-derived DOC and microbial necromass and products can also stabilize by direct bonding with soil minerals (Six et al., 2002; Six et al., 2006; Kleber et al., 2015). By binding to minerals through direct sorption or via microbial turnover (reviewed by Sokol et al., 2019), residue-derived SOC is believed to be highly inaccessible from enzymatic attack, resulting in its perceived long-term stability (Kögel-Knabner et al., 2008; Kleber et al., 2015). In contrast, residue that has been fragmented and physical transferred into the mineral soil is considered to have a shorter-term stability (Cotrufo et al., 2015), unless it is occluded in aggregates (Haddix et al., 2020), thus relying upon aggregation for protection from further decomposition (Cambardella & Elliott, 1992).

The amount of residue C that is microbially processed, and thus has greater potential to be stabilized by mineral association, may depend on the size of microbial biomass, which is largely a function of accessibility to substrate and protection from predation (Six et al., 2006). NT has repeatedly shown higher levels of microbial biomass compared to CT (reviewed by Strickland & Rousk, 2010; Van Groenigan et al., 2010), suggesting more potential for mineral-binding and longer-term C stabilization. The composition of the microbial community may also affect residue C stabilization, as it has been suggested that different microbial groups have different efficiencies of SOC formation (Bossuyt et al., 2001). Particularly, fungi, namely saprotrophs, are more equipped to degrade structural and more recalcitrant compounds, whereas bacteria favor low molecular weight and soluble compounds (Boer et al., 2005; Carney et al., 2007). Additionally, fungi are considered to have greater carbon to nitrogen ratios (C:N) than bacteria, indicating that fungi require less N per unit C for biomass formation (Paul, 2014). Due to the

suggested greater efficiency of fungal decomposition, fungal dominance has been linked to greater C stabilization (Jastrow et al., 2007).

Conventional tillage has been reported to decrease fungal to bacterial ratios (F:B) compared to NT (Beare et al., 1992; Frey et al., 1999), which may reduce the efficient breakdown of high C:N substrates that are more preferential for fungal decomposition (Carney et al., 2007). This shift in F:B may be the result of a high susceptibility of fungi to be harmed by physical disturbance and the lower utility of fungal feeding methods once residue is incorporated into the soil (Hendrix et al., 1986; Holland & Coleman, 1987) in comparison to bacteria. Furthermore, differences in soil moisture caused by tillage regime (Frey et al., 1999) may affect the shift in F:B. Yet, studies utilizing phospholipid fatty acids (PLFA's), which are components of microbial membranes that can differentiate microbial groups and serve as a proxy to determine F:B (Frostegård & Bååth, 1996), have indicated no difference in F:B between NT and CT (reviewed by Strickland & Rousk, 2010). Rather, PLFA analysis has indicated an increase in total microbial biomass with NT compared to CT, corresponding with an increase in SOC stabilization (reviewed by Strickland & Rousk, 2010; Van Groenigan, 2010).

Residues can be protected from microbial decomposition within aggregates (Six et al., 2002). In agroecosystems, aggregates play a particularly critical role in occluding residue and SOC, as well as microbial communities; however, stability depends on aggregate size (Trivedi et al., 2015). In particular, microaggregates (250 – 53 um) contribute to the longer-term stabilization of C than macroaggregates (>2000 – 250 um) (Jastrow et al., 2007), with mean residence times of C estimated to be approximately .8-4 years in macroaggregates and 7 years in microaggregates (Buyanovsky et al., 1994). These differences are attributed to the idea that macroaggregates are primarily stabilized through the enmeshment of fungal hyphae, roots, and transitory binding

agents, while microaggregates (250 – 53 um) seem to be formed by persistent microbial and elemental binding agents (Tisdall & Oades, 1982). As a result, macroaggregates are more vulnerable to disturbance (e.g. tillage) than microaggregates, leading to average turnover times of 30 and 88 days, respectively (De Gryze et al., 2006). Yet, microaggregates can be formed within and hatched from macroaggregates; therefore, the faster macroaggregate turnover that can be induced by the physical disturbance of tillage also inhibits new microaggregate formation (Six et al., 1998; 2004; Six & Paustian, 2014).

Ultimately then, aggregate dispersion from tillage, wet-dry cycles, or rain events can trigger pulses of microbial decomposition due to increased microbial accessibility to substrate (Elliott & Coleman, 1988; Balesdent et al., 2000), in effect, promoting immediate SOC formation and aggregation. However, this SOC may have poor potential to be ultimately stabilized within microaggregates. In particular, the repeated disturbance associated with tillage increases macroaggregate turnover and, thus, inhibits microaggregate formation (Six & Paustian, 2014). With a lesser ability for SOC to be occluded within microaggregates, the repeated disturbance associated with CT will trigger further disruption of macroaggregates and microbial decomposition of unprotected SOC. As a result, the interplay between aggregate formation and disruption induced by CT may decrease the amount of residue-derived SOC recovered in the soil in the long-term due to increased CO_2 respiration.

To understand the mechanisms responsible for the interactive effects of tillage on SOC dynamics, it is necessary to disentangle disturbance from residue incorporation. Several studies have specifically examined residue location placement (i.e., incorporated vs. surface-applied) and found that, initially, the incorporation of residue increases both residue decomposition and residue-derived SOC accrual (Leichty et al., 2020); however, over time, differences in residue-

derived SOC accrual subside (Mitchell et al., 2018). To understand this result, we continue the experiment from Leichty et al. (2020) and quantify the biological and physical parameters affecting decomposition throughout a 30-month study period. Using isotopically labeled ^{13}C residue, we tracked the effects of residue incorporation vs. surface application on residue-derived C dynamics (i.e., SOC formation efficiency), soil aggregation, as well as on microbial biomass, composition, and enrichment using compound-specific stable isotope probing (via PLFA-C). We hypothesized that (1) residue incorporation (INC) will initially result in a greater residue-derived fungal-dominated soil microbial community than surface-application of residue due to differences in substrate availability. As a result, we expect that INC will demonstrate more efficient residue-derived SOC formation and greater residue-derived SOC accrual in the short-term. However, over time, we hypothesize that (2) repeated disturbance and weak aggregate stability in INC will result in continued substrate availability and microbial decomposition, and thus less efficient residue-derived SOC formation due to continued CO_2 loss. In contrast, we expect the surface-applied residue treatments to increase in residue-derived fungal dominance as structural residue physically moves down through the soil profile, resulting in more efficient residue-derived SOC formation and greater protection from microbial decomposition due to lack of disturbance in the longer-term. Thus, we hypothesize that differences in residue-derived SOC accrual between treatments will subside after 30 months.

CHAPTER 2: MATERIALS AND METHODS

2.1 Experimental Site

This field experiment was conducted at the Colorado State University's Agricultural Research, Development and Education Center (ARDEC), located approximately 10 km northeast of Fort Collins, Colorado (40° 39' 6" N, 104° 59' 57" W; 1535 m above sea level). This climate of this site is considered semiarid, with a mean annual temperature of 10.1°C and mean annual precipitation of 408 mm (Leichty et al., 2020)

The research site is under irrigated, historically continuous no-till corn, where the soil is classified as a Fort Collins clay loam (fine-loamy, mixed, mesic Aridic Haplustalf). The site is well documented and described in detail in Halvorson & Stewart (2015) and Leichty et al., (2020). Each year, corn (*Zea mays L.*) is approximately planted in May and harvested in November. A single dose of fertilizer high efficiency fertilizer (46% urea N) is surface-band applied once per year at a rate of 135 kg N ha^{-1} and approximately 35 mm of irrigation water is sprinkled once a week during the growing season (Leichty et al., 2020).

2.2 Experimental Design

This experiment was conducted over a period of 30 months, from November 2017 to May 2020. It consists of 4 rows of 10 cm diameter PVC collars, which were split into two sets: one for continuous gas sampling and one for destructive soil harvest. The gas sampling set is designed as a randomized complete block design with 5 treatments and 4 replicates, for a total of 20 collars. The second set for destructive soil harvest is also designed as a randomized complete block design, with 3 plots each corresponding to a harvest date (6, 12, and 30 months post-establishment). Each plot has 3 treatments and 4 replicates, for a total of 12 collars per plot.

A detailed presentation of the experimental design can be found in Leichty et al. (2020). Briefly, big bluestem residue with a ^{13}C label of 3088‰ was added either on the soil surface (SA) or incorporated into the soil (INC). An additional treatment (SA-NR) was established to separate the effects of residue incorporation from those of physical disturbance. Control treatments (C-SA and C-INC) to obtain isotopic background values for gas measurements were similarly handled, but received unlabeled corn stover. Table 1 provides an explanation of each treatment and how each treatment was altered after 12 months, at which point we simulated an annual harvest. Due to poor weather conditions, there was no successive harvest simulation at 24 months.

Table 1. An explanation of treatments. Treatment name corresponds to the abbreviation used to differentiate each treatment. Collar set corresponds to whether treatment is present in the gas sampling collar set, destructive harvest collar set, or both. Residue placement describes whether residue was surface-applied or incorporated into the soil. Two harvest events took place, one at 0 months and one at 12 months, represented by 0 month harvest and 12 month harvest, respectively. Harvest events were characterized by disturbance (i.e., soil was disturbed or undisturbed) and residue addition (i.e., whether ^{13}C labeled *Andropogon gerardii*, unlabeled corn stover, or neither were added).

			0 Month Harvest		12 Month Harvest	
Treatment Name	**Collar Set**	**Residue Placement**	**Disturbance**	**Residue Addition**	**Disturbance**	**Residue Addition**
INC	Gas Sampling and Destructive Harvest	Incorporated	Disturbed	^{13}C labeled *Andropogon gerardii*	Disturbed	Unlabeled corn stover
SA	Gas Sampling and Destructive Harvest	Surface Applied	Undisturbed	^{13}C labeled *Andropogon gerardii*	Undisturbed	Unlabeled corn stover
SA-NR	Gas Sampling and Destructive Harvest	Surface Applied	Disturbed	^{13}C labeled *Andropogon gerardii*	Undisturbed	None
C-INC	Gas Sampling	Incorporated	Disturbed	Unlabeled corn stover	Disturbed	Unlabeled corn stover
C-SA	Gas Sampling	Surface Applied	Undisturbed	Unlabeled corn stover	Undisturbed	Unlabeled corn stover

2.3 CO_2 Sampling

Gas sampling was performed throughout the entire duration of this experiment, from twice a week (before and after weekly irrigation) during the growing season to once a month during the winter. A more detailed explanation of the procedure is provided in Leichty et al. (2020), but briefly, collars were sealed at each sampling and 45 mL of headspace was extracted every 15 minutes over a 45-minute sampling period (0, 15, 30, and 45 minutes). Each sample was analyzed on a gas chromatograph (GC; Varian 450 coupled to a thermal conductivity detector; Varian Inc., CA) for CO_2 and on an isotope ratio mass spectrometer (IRMS; stable isotope analyzer continuous flow isotope ratio mass spectrometer coupled to a Gilson CO_2 gas autosampler; Europa Scientific, England) for isotopic $\delta^{13}CO_2$.

2.4 Soil Sampling and Processing

Upon establishment of the experiment, a Gidding's rig with a 6.25 cm diameter coring tube was used to extract 100 cm soil cores from both the north and south sides of each row. The north and south soil cores of each row were combined to create a cumulative baseline representation of every row, for a total of 4 cumulative baseline samples. Cumulative baseline samples were divided into their respective 0-5 and 5-10 cm depths.

At each timepoint (6, 12, and 30 months after establishment), 12 collars were destructively harvested. Collars were carefully dug out of the ground, each placed in a plastic bag, and stored in a cooler. Collars were brought back to the laboratory the same day, upon which soil cores were carefully extracted from within collars, divided into their respective 0-5 and 5-10 cm depths, and weighed. Any undecomposed residue remaining on the surface of the samples was removed and dried in a 55°C forced air oven. Soil samples were hand-homogenized and sub-

sampled to measure soil moisture. Bulk densities of soil samples were calculated using gravimetric water content, rock weight, and core volume, according to Blake (1965).

Within two months after sampling, all soil processing was complete. Briefly, samples were gently passed through an 8 mm sieve without compromising aggregate structure and handpicked to remove plant material and rocks. Subsamples were taken for aggregate fractionation and air dried for several weeks. Additional subsamples of 8 mm sieved soil were passed through a 2 mm sieve, hand-picked to remove additional plant material and rocks, air-dried, and ground for elemental analysis. Further subsamples of 8 mm sieved soils were processed for microbial analyses, in which subsamples were thoroughly handpicked to remove any visible plant material or rock, frozen in a -20°C freezer, and freeze-dried (Labconco FreeZone 77530, Kansas City, MO). Freeze-dried samples were stored at room temperature until extraction during May-September 2020. The remainder of the 8 mm sieved soil was stored in a 3°C freezer. All removed plant material was combined per soil sample, dried in a 55°C forced air oven, and ground for elemental analysis.

2.5 Aggregate Size Fractionation

Aggregate fractionation was performed on 0-5 and 5-10 cm samples as described by Figure 1. After gentle rewetting, the 8 mm subsamples were wet sieved for 45 minutes using a Yoder apparatus (ref) in conjunction with a 2 mm and 250 um sieve, resulting in > 2000 um (large macroaggregates), 250 – 2000 um (small macroaggregates), and 0 – 250 um fractions. The 0 – 250 um fraction was additionally passed through a 53 um sieve using a stream of deionized water, resulting in 53 – 250 um (microaggregates) and <53 um (silt- and clay-sized particles) fractions. Flocculent ($MgCl_2$) was added to the <53 um fraction to speed up the settling of the soil. The soil settled within one week, at which point most of the water was decanted. Floating

detritus was removed from each fraction. All aggregate size fractions were dried in a 55°C oven, weighed, and stored at room temperature. Dried weights of aggregate size fractions were used to confirm a 100 ± 3% percent recovery for each sample. Furthermore, weights were used to calculate the mean weight diameter (MWD) of each sample, using the equations (1) and (2):

(1) $$MWD = \Sigma P_f S_f$$

(2) $$P_f = \frac{w_f}{w_i}$$

where P_f is the proportion of the *f*th fraction in the initial sample, S_f is the average diameter of aggregates in the *f*th fraction, w_f is the weight of the *f*th fraction, and w_i is the weight of the initial sample.

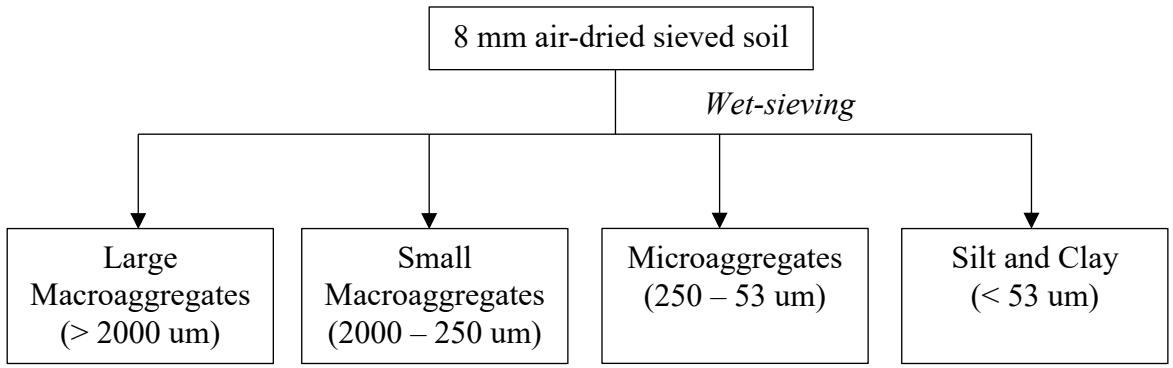

Figure 1. Schematic representing the aggregate fractions that were obtained from 8mm air-dried sieved soil using wet-sieving (revised from Gillabel et al., 2007).

2.6 Phospholipid Fatty Acid Extraction and Quantification

Fatty acids, which are microbial biomarkers that can be used as a proxy to analyze microbial community, were extracted from 0-5 and 5-10 cm samples using an adapted method of Bossio and Scow (1995), modified by Denef et al. (2007). Briefly, 6g subsamples of freeze-dried 8mm soils were dispersed in a final solution of 0.9:1:1 of potassium phosphate buffer:chloroform: methanol. Phospholipid fatty acids (PLFA's), neutral lipid fatty acids (NLFA's), and glycolipids

were isolated from the chloroform layer through silica gel solid-phase extraction (SPE) columns by using methanol, acetone, and chloroform as eluents, respectively. Glycolipids were discarded, while PLFA's and NLFA's were transesterified to form fatty acid methyl esters (FAME's). FAME's were isolated under N_2 and frozen in a -20°C freezer. Days before being run for analysis, FAME's were reconstituted with a 150 uL addition of hexane and a 150 uL addition of a C12:0 and C19:0 internal standard solution.

Reconstituted samples were injected (1-3 uL) into a capillary gas chromatography-combustion-isotope ratio mass spectrometer (GC-c-IRMS; Trace GC Ultra coupled to GC Isolink, ConFlo 4 Interface Unit, and Delta V Advantage; Thermo Scientific, Germany), with a column length of 60m. The temperature program ran as follows: after a one-minute hold at 100°C, the temperature ramped up to 190°C at 20°C min^{-1}, then transitioned to a temperature ramp of 1.5°C min^{-1} until the temperature reached 235°C, after which the temperature ramped up to 295°C at 20°C min^{-1}, with a final 10-minute hold at 295°C.

To identify each peak to its corresponding FAME compound, retention time ratios were calculated (retention time of peak:retention time of C12:0 standard) and compared to those of known external standards (FAME37 and BAME, Supelco Inc.). To account for the addition of the methyl group that occurs during transesterification, measured $\delta^{13}C$ values for each FAME were corrected using simple mass balance (Denef et al., 2007).

Reconstituted FAME's were then injected (1 uL) into the gas chromatograph-mass spectrometer (GC-MS; Shimadzu QP-20120SE) with a column length of 30m. The temperature program ran as follows: starting at 100 °C, the temperature ramped up to 160 °C at a heating rate of 30 °C min−1, after which it ramped up to 280 °C at 5 °C min−1. Peaks were identified to their corresponding FAME compounds by using the NIST-2011 Mass Spectral Library. To quantify

the peaks, relative response factors (RRF's) were calculated for each FAME compound using C19:0, FAME37, and BAME (Suplco Inc.). RRF's were used to calculate ng PLFA C g^{-1} soil, a proxy for microbial biomass, of each FAME compound. To estimate total soil microbial biomass of a sample, the microbial biomass of each biomarker within a sample was summed together. Mol percentages were calculated based on the individual biomass of a biomarker divided by the total microbial biomass of the sample, and then used to represent soil microbial composition.

Fatty acid nomenclature follows standard protocol (A:BωD), in which the A corresponds to number of C atoms, the B corresponds to the number of double bonds, and the D corresponds to the C atom on which the double bond located (Kong et al., 2011). Furthermore, OH corresponds to a hydroxyl group, Me corresponds to a methyl group, cy corresponds to a cyclopropane group, a- corresponds to anteiso-branched fatty acids, and i- corresponds to iso-branched fatty acids. FAME compounds were identified by their general microbial group as follows: gram-negative bacteria are represented by 2OH 10:0, 2OH 12:0, 2OH 14:0, 2OH 16:0, 17:0cy, 19:0cy, 16:1ω7, and trans-18:1ω7; gram-positive bacteria are represented by i-15:0, a-15:0, i-16:0, i-17:0, and a-17:0; actinomyces are represented by 10Me16:0, 10Me17:0, and 10Me18:0; general bacteria are represented by 3OH 12:0, 3OH 14:0, 14:0, 15:0, 17:0, and 18:0; arbuscular mycorrhizal fungi (AMF) are represented by 16:1ω5, 20:4ω6, 20:5ω3, and 20:1; saprotrophic fungi are represented by 18:3ω6, 18:2ω6, and cis-18:1ω7; universal microbes are represented by 16:0. Undefined bacteria are not included in our calculations for microbial biomass or composition, but are represented by 10:0, 11:0, 13:0, 14:1, 15:1, 17:1, 20:0, 20:2, 20:3ω3, 20:3ω6, 21:0, 22:0, 22:1ω9, 22:2, 22:6ω3, 23:0, 24:0, and 24:1.

2.7 Carbon Analysis

Bulk soil (i.e., 2 mm sieved soil) and plant material were weighed into tin capsules in duplicates. To account for inorganic carbonates in our bulk soil, a duplicate of each sample was acidified by placing the tin capsule into a desiccator alongside a beaker of hydrogen chloride. Both the acidified and unacidified replications were run on the isotope ratio mass spectrometer (IRMS; stable isotope analyzer continuous flow isotope ratio mass spectrometer coupled to a Gilson CO_2 gas autosampler; Europa Scientific, England) and analyzed for %C and $\delta^{13}C$.

2.8 Data Analysis

A two-end member mixing model was used to partition residue-derived C from total C. The f-value, determined by equation 3, represents the proportion of residue-derived C within the sample and can be multiplied by the weight of the total sample in order to calculate the weight of the residue-derived C in the sample.

(3) $$f - value = \frac{\delta_S - \delta_C}{\delta_R - \delta_C}$$

where δ_S, δ_C, and δ_R is the ^{13}C of the sample, ^{13}C of the control, and ^{13}C of the initial residue, respectively.

SOM formation efficiency was calculated by dividing the total amount of residue-derived C recovered as residue in the soil by the amount of residue C lost. Residue C lost was calculated by subtracting the residue C recovered as residue by the initial amount of residue C added (Haddix et al., 2016).

Residue-derived carbon recovery was calculated by dividing the sum of all of the residue C recovered (SOC, soil inorganic C, CO_2, and residue C) by the initial amount of residue C added (3088 kg C ha^{-1}).

Given bulk density values at the 30-month harvest were not reliable, we generated a more accurate estimate by averaging the 0, 6, and 12 month bulk densities values by treatment and depth layer to represent the 30 month bulk density.

2.9 Statistical Analysis

A linear fixed-effects model, using replicate as a random effect and Tukey adjustments, was used to compare the effects of treatment and timepoint on residue-derived CO_2 respiration, residue-derived soil C, aggregation, residue-derived soil microbial biomass, and residue-derived soil microbial composition. Pearson correlations were used to compare MWD versus residue-derived bulk C and SOC formation efficiency versus residue-derived F:B. Residual diagnostic plots were used to evaluate normality. Comparisons were considered significant at the p=.05 level. Analyses were performed using R Studio Version 1.3.1093.

Outliers for CO_2 data were assessed by whether values were within the average ± 3 standard deviations; values outside this range were considered outliers and replaced by the mean of the other three values, in order to maintain consistency with previous statistical analyses of this data. One MWD value was considered an outlier because the percent recovery was outside the range of 97-103%; this outlier replaced by the mean of the other three MWD values. Twenty-one PLFA measurements were considered outliers and removed because deltas were considered unrealistic (less than -30 ‰). To precisely calculate baseline control values for PLFA's, forty-two baseline PLFA's were considered outliers and removed because they were outside the range of the mean ± 3 standard deviations.

CHAPTER 3: RESULTS

3.1 Residue-Derived Carbon Recovery

There were clear treatment differences in amounts of residue-derived soil organic C (SOC) recovered in the mineral soil, particularly at 6 and 12 months (Table 2). At 6 months, the incorporated treatment (INC) retained nearly twice as much residue-derived SOC as the surface-applied (SA) treatment and slightly over three times as much residue C as the surface applied/no new residue (SA-NR) treatment ($p= 0.0088$ and $p=.0001$, respectively). At 12 months, INC continued to retain more residue-derived SOC than the surface-applied treatments, although the difference between treatments was not as large. Specifically, INC contained 1.5 times as much residue-derived SOC as SA and nearly twice as much residue-derived SOC as SA-NR ($p= 0.0015$ and $p <.0001$, respectively). At 30 months, INC retained more residue-derived organic C than surface-applied treatments, although this was not significant.

From 6 to 12 months, all treatments exhibited a significant increase in amount of residue-derived organic C recovered in the mineral soil (Table 2). Specifically, INC retained over 59% more residue-derived SOC, SA retained 98% times more residue-derived SOC, and SA-NR retained 163% more residue-derived SOC at 12 months than it did at 6 months ($p=.0008$, $p=.005$, and $p=.0035$, respectively). SA and SA-NR exhibited a further increase in residue-derived SOC retained from 12 to 30 months (13% and 52%, respectively), but this was only significant for SA-NR ($p=.0221$), whereas INC retained 3% less residue-derived SOC at 30 months than it did at 12 months, although this difference was not statistically significant.

Residue-derived inorganic C recovered in the mineral soil was variable, but not statistically different across both treatments and time (Table 2).

While INC lost more residue-derived C as CO_2 after 6 months than the surface-applied treatments, SA and SA-NR lost more residue-derived C as CO_2 than did INC over the course of 30 months (Table 2; Figure 2). Specifically, INC lost over twice as much residue-derived CO_2 as did either SA or SA-NR at 6 months, although this was not significant. At 12 months, SA and SA-NR lost 29% and 18% more residue-derived CO_2 than did the incorporated treatment (INC), with differences only being significant between INC and SA ($p=.0078$). At 30 months, the cumulative residue-derived C lost as CO_2 was 39% and 28% greater for SA and SA-NR, respectively, than INC ($p<.0001$ and $p=.003$, respectively).

Temporal differences within treatments were significant for INC, SA, and SA-NR from 6 to 12 months ($p<.0001$, $p<.0001$, and $p<.0001$, respectively) (Table 2). From 12 to 30 months, the change in residue-derived C lost as CO_2 was only considered significant for SA and SA-NR ($p=.0115$ and $p=.0204$, respectively). All treatments demonstrated high rates of residue-derived CO_2 respiration upon establishment and during growing seasons (Figure 2). INC lost more residue-derived CO_2 than SA and SA-NR upon establishment, while SA and SA-NR had greater residue-derived CO_2 fluxes than INC did during growing seasons.

More residue C was recovered as residue in surface-applied treatments than in INC for all timepoints (Table 2; Figure 3). At 6 months, there was 2.3 and over 2 times as much residue C recovered in SA and SA-NR, respectively, as there was in INC ($p=.0005$ and $p=.0037$, respectively). At 12 months, SA had over 10 times and SA-NR had nearly 8 times as much residue C as did INC ($p<.0001$ and $p<.0001$). Differences in residue C recovered were not significantly different at 30 months, although surface-applied treatments continued to retain more residue C. While INC had less residue C recovered from 6 to 12 months (not significant), SA and

SA-NR had significantly less residue C recovered from 12 to 30 months (p=.0007 and p=.0001, respectively).

Total residue C recovered was variable across treatment and timepoint, ranging from 40-70% residue C recovered (Table 2). Greatest residue C recovery occurred at 12 months for all treatments.

The percentage of residue C initially added that remained in residue was similar for SA and SA-NR throughout the duration of the experiment, while INC consistently had less residue C remaining compared to surface-applied treatments (Figure 3).

Table 2 Cumulative residue-derived carbon (in kg C ha^{-1}) recovered in soil organic carbon, and soil inorganic carbon, CO_2, and residue for INC (incorporated residue), SA (surface-applied residue) and SA-NR (surface-applied residue without new residue addition) treatments from 0-100 cm. Total residue C recovered was calculated by dividing the sum of all of the residue C recovered (SOC, soil inorganic C, CO2, and residue C) by the initial amount of residue C added (3088 kg ha-1). Timepoint corresponds to soil core harvest times (i.e., 6, 12, and 30 months after establishment of experiment). Data represent averages and standard errors (n=4).

Treatment		INC			SA			SA-NR		
Timepoint		6	12	30	6	12	30	6	12	30
Initial Residue Added (kg C ha^{-1})		3088	3088	3088	3088	3088	3088	3088	3088	3088
Residue C Recovered (kg C ha^{-1})	Soil Organic C	556 ± 51	883 ± 43	853 ± 19	288 ± 54	571 ± 105	645 ± 49	179 ± 20	470 ± 46	713 ± 44
	Soil Inorganic C	28 ± 14	11 ± 11	20 ± 16	10 ± 10	18 ± 7	13 ± 3	16 ± 10	9 ± 6	41 ± 18
	CO_2	237 ± 18	543 ± 31	613 ± 33	114 ± 3	702 ± 32	854 ± 32	113 ± 5	643 ± 37	786 ± 38
	Residue	446 ± 88	82 ± 13	34 ± 10	1046 ± 147	848 ± 74	266 ± 68	950 ± 83	877 ± 98	190 ± 28
Total Residue C Recovered (%)		41	49	49	47	69	58	41	65	56

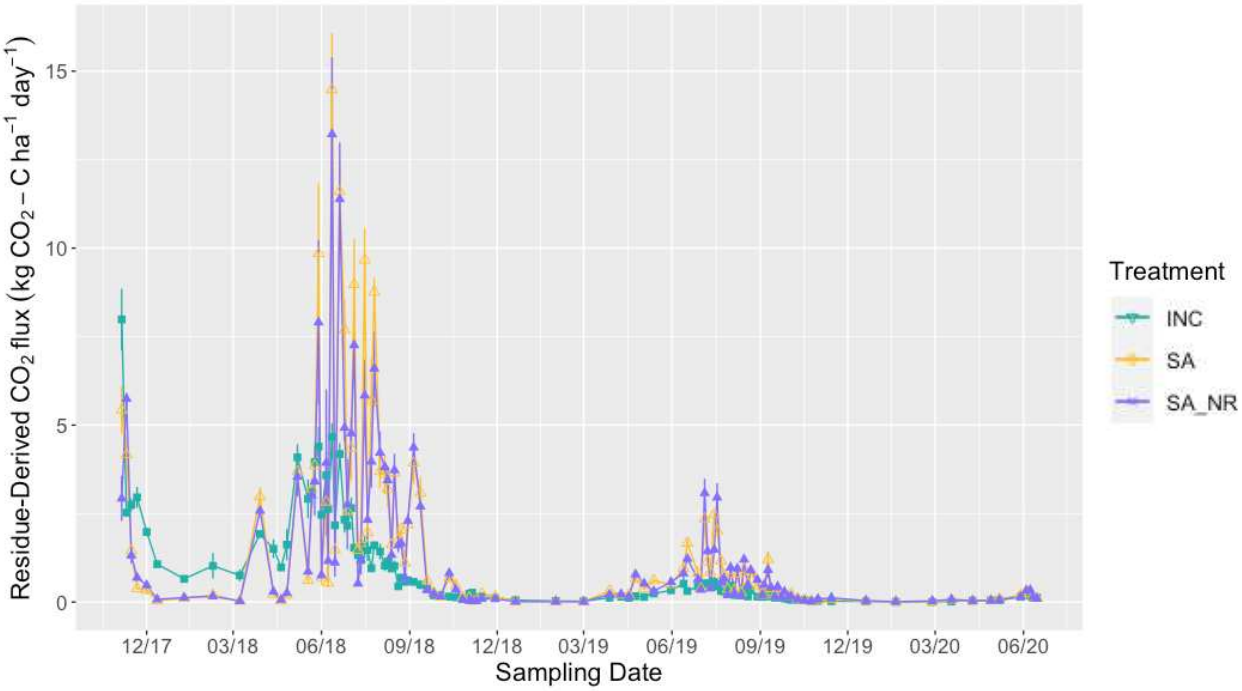

Figure 2. Residue-derived CO_2 flux (kg CO_2-C ha^{-1} day^{-1}) of incorporated (INC), surface-applied (SA), and surface-applied/no new residue (SA-NR) treatments over 30 months.

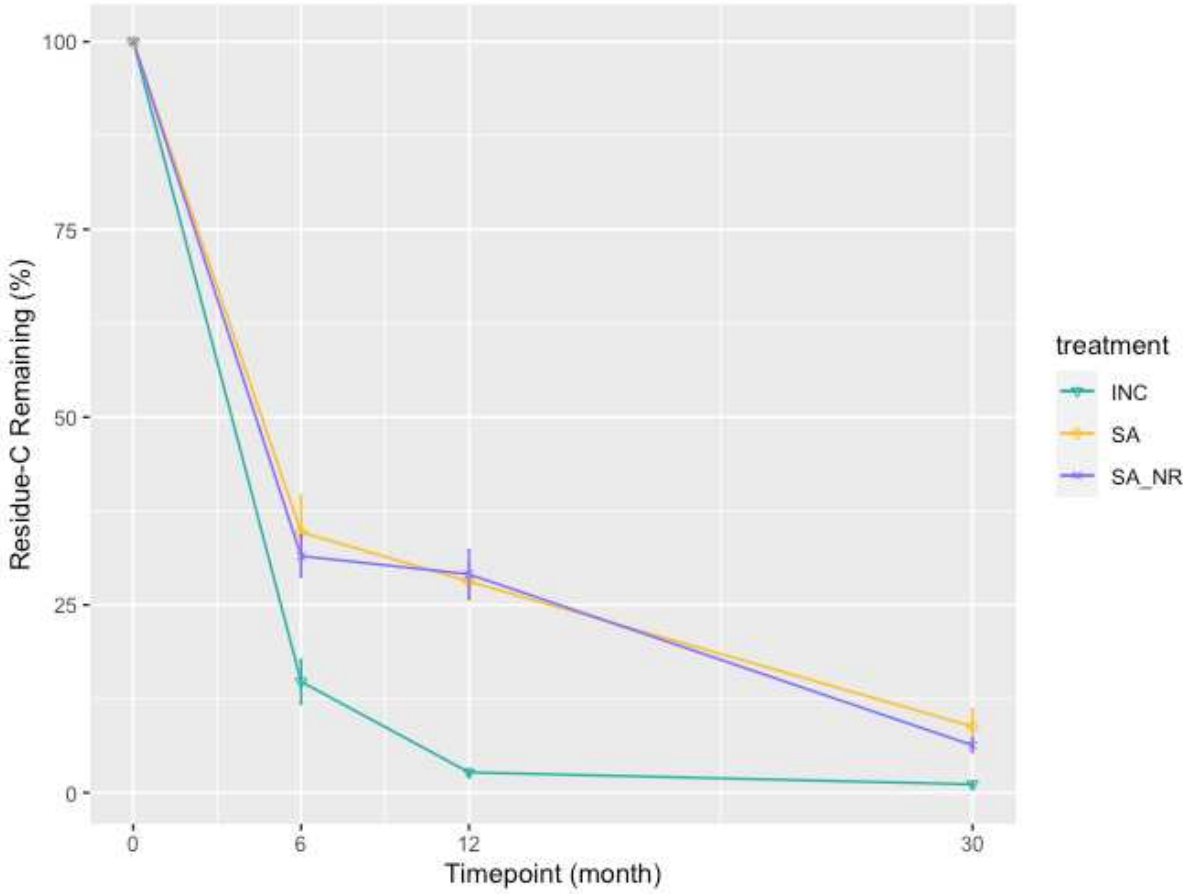

Figure 3. Residue carbon (C) remaining (%) for incorporated (INC), surface-applied (SA), and surface-applied/no new residue (SA-NR) treatments for 0-10 cm at all soil core harvest times (i.e., 6, 12, and 30 months after establishment of experiment). Data represent averages and standard errors (n=4)

3.2 Soil Organic Carbon Formation Efficiency

Average SOC formation efficiencies from residue decomposition were calculated for incorporated (INC) versus surface-applied (SA and SA-NR) (Figure 4). After 6 months, the incorporated residue treatment was approximately twice as efficient in SOC formation than surface-applied residue treatments ($p=.0007$). After 12 months, INC was still significantly more efficient than surface-applied residue treatments, but not as drastically as at 6 months ($p=.0406$). SOM formation efficiencies were not significantly different depending on residue placement after 30 months. From 6 to 12 months, both incorporated and surface-applied treatments increased in SOC formation efficiencies ($p=.0213$ and $p<.0001$, respectively).

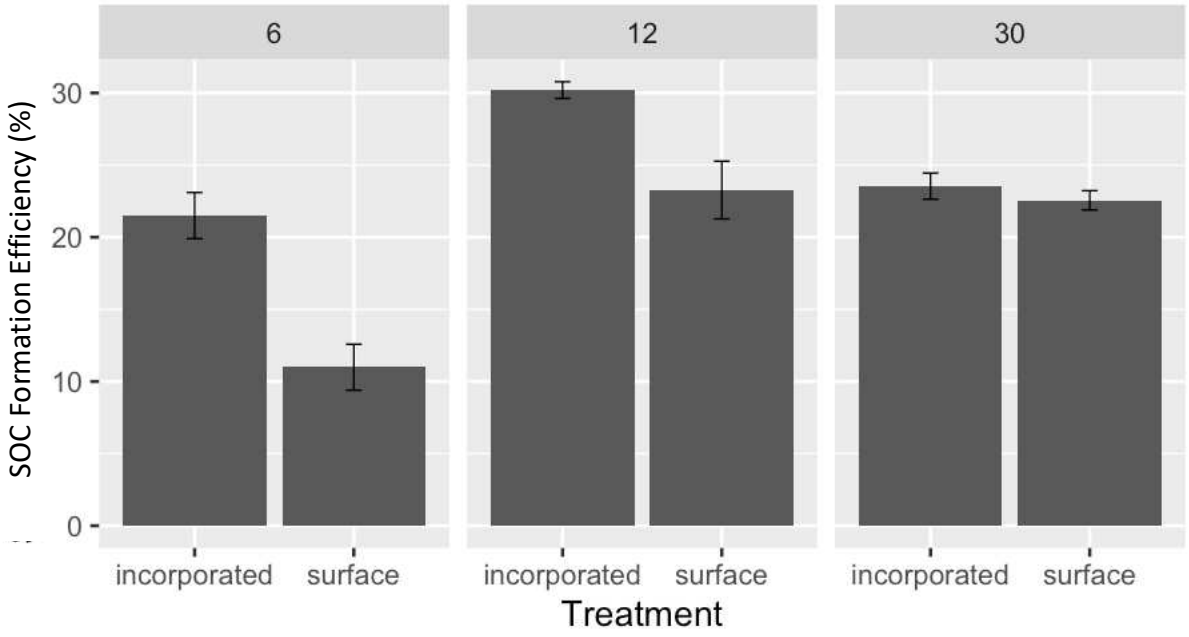

Figure 4. Soil organic carbon (SOC) formation efficiencies (%) for incorporated (INC) versus surface (surface-applied; SA and SA-NR) treatments for 0-10 cm. Panels correspond to soil core harvest times (i.e., 6, 12, and 30 months after establishment of experiment). Data represent averages and standard errors (n=4 for incorporated and n=8 for surface).

3.3 Aggregate Mean Weight Diameter

Across time, all treatments followed a similar seasonal trend, in which aggregate mean weight diameters (MWD's) were generally smaller at spring harvests (6 and 30 month) and larger at fall harvest (12 month) (Figure 5).

At the 0-5 cm depth, there were no apparent treatment differences in MWD at any timepoint (Figure 5). All treatments, however, exhibited temporal changes in MWD. From 6 to 12 months, INC, SA, and SA-NR increased in MWD by 65%, 41% and 62%, although changes were not significant. From 12 to 30 months, INC and SA-NR decreased in MWD by 45% and 54% ($p=.0279$ and $p=.0017$), while SA stayed approximately the same.

At the 5-10 cm depth, temporal differences were less pronounced than those seen in the 0-5 cm depth, while treatment differences were present (Figure 5). Only the surface applied treatments (SA and SA-NR) appeared to have significant temporal differences in MWD. Particularly, the MWD of SA decreased by 51% from baseline to 6 months ($p=.0737$), while the MWD of SA-NR increased by 124% from 6 months to 12 months ($p=.0027$). At 6 months, INC had 121% larger MWD than SA ($p=.0282$), while differences in MWD between INC and SA-NR at 6 months were not significant. Significant differences between disturbed (INC and SA-NR) and undisturbed (SA) treatments were apparent at 12 months. At 12 months, the MWD's of INC and SA-NR were 95% ($p=.0348$) and 123% ($p=.00277$) larger than that of SA, respectively. At 30 months, there were no significant differences present between treatments.

Correlations between MWD and residue-derived SOC content indicated a relatively strong relationship in incorporated residue treatments ($r^2=.34$, $p=.0029$), compared to no relationship in surface-applied residue treatments ($r^2=.03$, $p=.21$) (Figure 6).

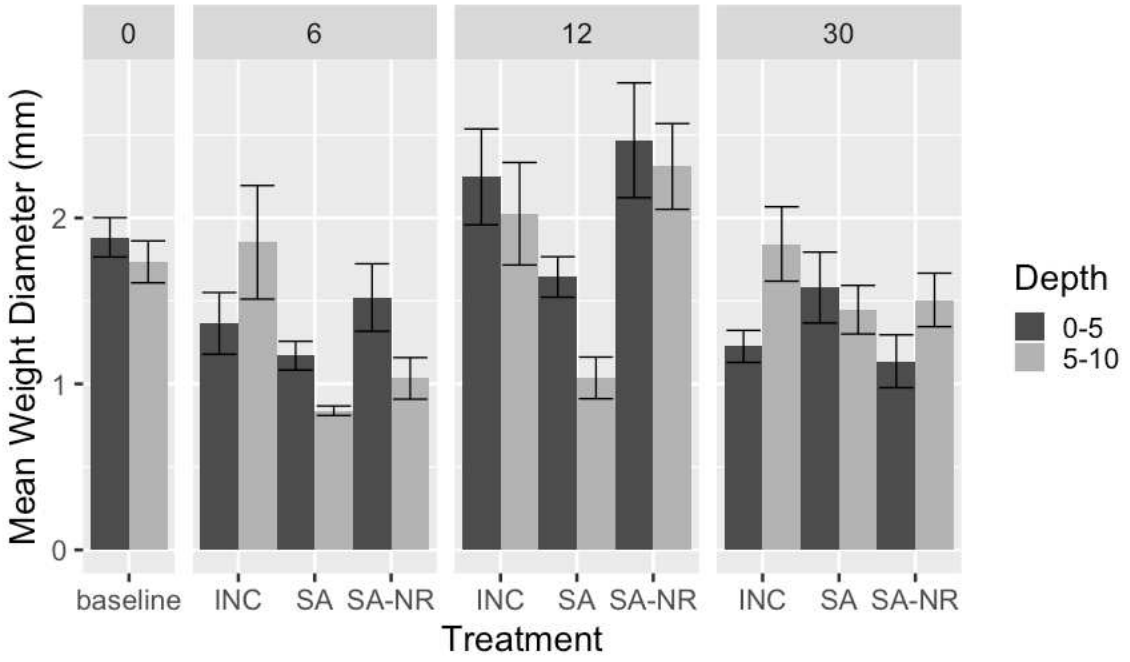

Figure 5. Mean weight diameters (mm) of 0-5 cm and 5-10 cm depths of baseline, INC (incorporated residue), SA (surface-applied residue), and SA-NR (surface-applied residue without new residue addition) treatments. Panels correspond to soil core harvest times (i.e., 6, 12, and 30 months post establishment of the experiment). Data represent averages and standard errors (n=4).

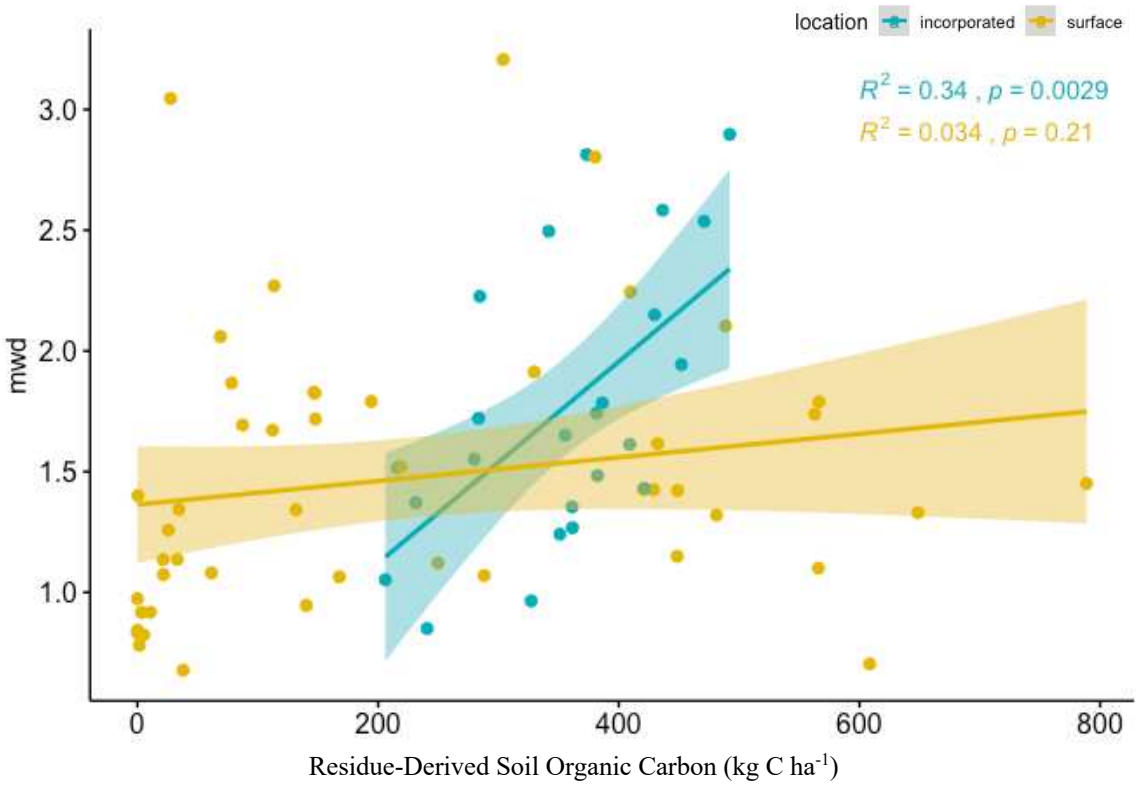

Figure 6. Correlation between mean weight diameter (MWD) (mm) and residue-derived soil organic carbon (kg C ha^{-1}) from 0-10 cm for incorporated (INC) and surface-applied (SA and SA-NR) residue treatments at all timepoints (n=24 for incorporated; n=48 for surface-applied).

3.4 Soil Microbes

The amount of residue-derived C recovered in microbes was estimated by determining the mass of ^{13}C labeled PLFA's using a mixing model (Figure 7). There were significant differences between INC and the surface-applied treatments (SA and SA-NR) at 6 and 12 months, whereas, after 30 months, there were no apparent differences between treatments. Specifically, INC had 109% and 140% greater residue-derived microbial biomass than SA and SA-NR at 6 months, respectively ($p<.0001$ and $p<.0001$), and 109% and 101% greater residue-derived microbial biomass than SA and SA-NR at 12 months, respectively ($p=.0001$ and $p=.0001$).

Over time, treatments had differing temporal trends in residue-derived soil microbial biomass (Figure 7). While SA-NR maintained a steady increase in residue-derived microbial biomass over time, both INC and SA decreased in biomass over time. The decrease in SA was not significant, whereas INC decreased by 22% from 6 to 12 months ($p=.0581$) and by 36% from 12 to 30 months ($p=.0056$).

No significant treatment differences in residue-derived fungal:bacterial ratio (F:B) existed except at 6 months, in which that of SA was greater than SA-NR ($p=.0034$) (Figure 8). At 0-5 cm, all treatments (INC, SA, and SA-NR) demonstrated a significant increase in residue-derived F:B from 6 to 12 months ($p<.0001$, $p=.0021$, and $p<.0001$, respectively) (Figure 7a). While the surface-applied residue treatments remained constant from 12 to 30 months, the incorporated residue treatment decreased in residue-derived F:B from 12 to 30 months, roughly back to 6 month values ($p=.0016$). At 5-10 cm, only SA-NR demonstrated any significant change in residue-derived F:B, particularly an increase from 6 to 12 months ($p=.0065$) (Figure 7b).

Correlations between residue-derived F:B and SOC formation efficiency indicated a strong relationship in incorporated residue treatments (r^2=.73, p<.0001), compared to a lesser relationship in surface-applied residue treatments (r^2=.38, p<.0001) (Figure 9).

A principle component analysis (PCA) of residue-derived microbial biomass indicated that, while depth was not a significant variable affecting residue-derived microbial composition, timepoint and treatment were (Figure 10). Several microbial biomarkers were particularly significant in differentiating early- versus later-stage microbial communities. Earlier microbial communities were significantly more abundant in gram-negative bacteria (trans-18:1ω7 and 16:1ω7), saprotrophs (cis-18:1ω7 and 18:2ω6), undefined microbes (17:1), and gram-positive bacteria (a-15:0). Later microbial communities were significantly more abundant in general bacteria (17:0, 18:0), gram-negative bacteria (17:0cy), gram-positive bacteria (i-15:0), and AMF (16:1ω5).

Several biomarkers were significant in separating disturbed (INC and SA-NR) versus undisturbed (SA) microbial communities (Figure 10). Particularly, disturbed treatments were characterized by general bacteria (17:0), gram-negative bacteria (17:0cy), gram-positive bacteria (i-15:0, i-17:0), and AMF (16:1ω5). Furthermore, the saprotrophic biomarker 18:2ω6 was significantly linked to INC in particular. Undisturbed treatments, on the other hand, were characterized by gram-negative bacteria (trans-18:1ω7), saprotrophs (cis-18:1ω7), and undefined microbes (17:1).

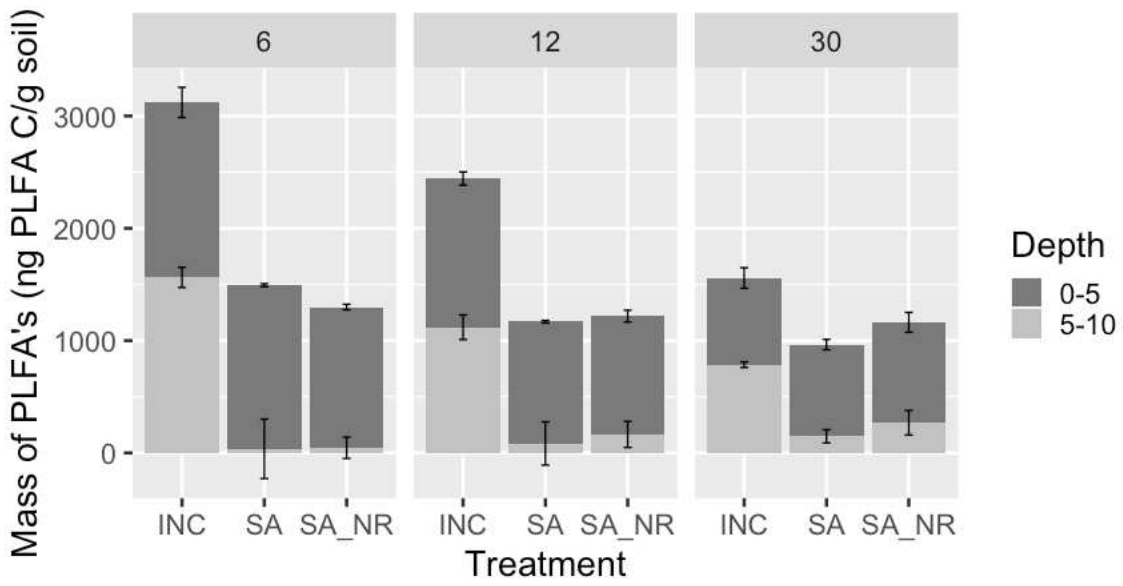

Figure 7. Residue-derived soil microbial biomass (ng PLFA C g^{-1} soil) across 0-5 cm and 5-10 cm of INC (incorporated residue), SA (surface-applied residue), and SA-NR (surface-applied residue without new residue addition). Total mass of PLFA-C was used as a proxy for total microbial biomass. Panels correspond to soil core harvest times (i.e., 6, 12, and 30 months post establishment of the experiment). Data represent averages and standard errors (n=4).

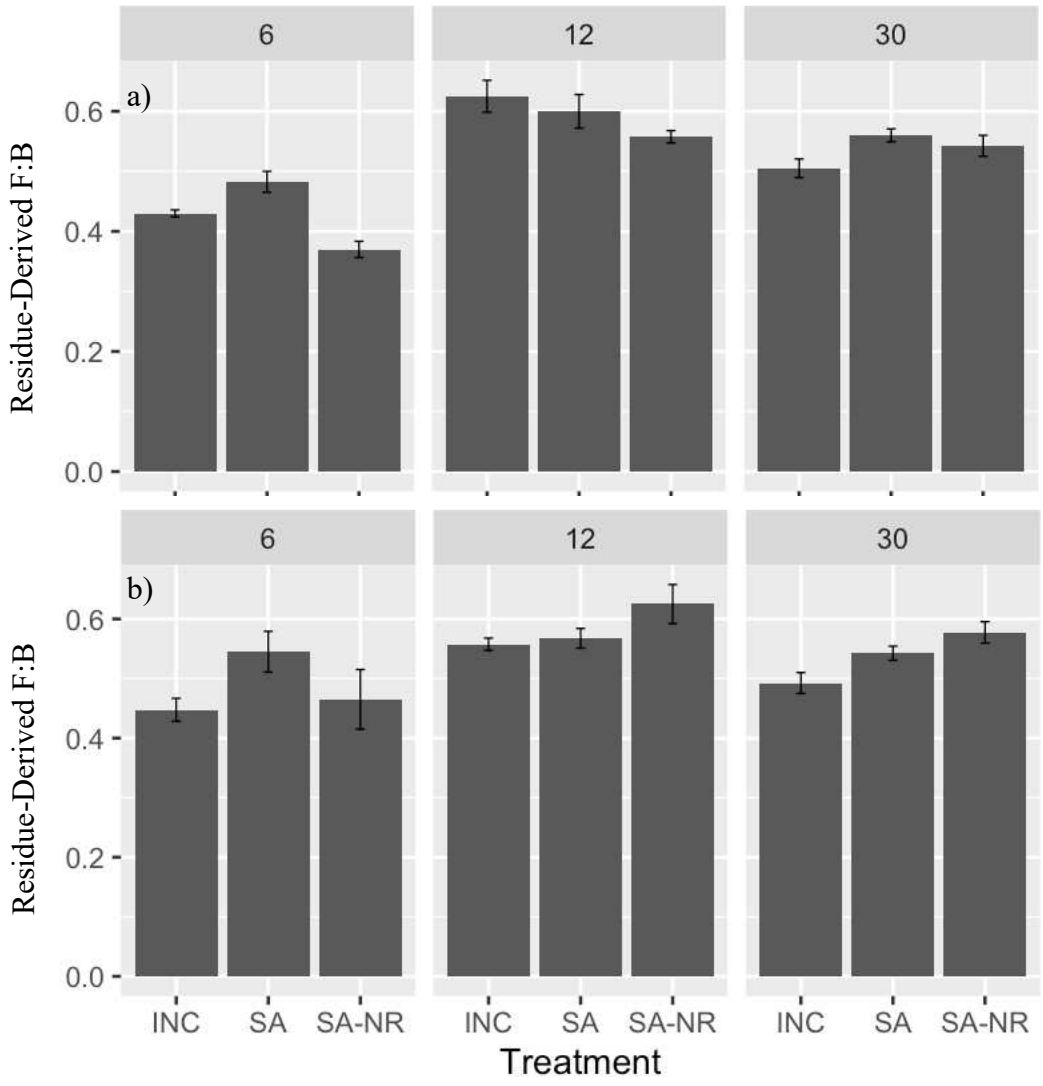

Figure 8. Residue-derived fungal C:residue derived bacterial C ratios (F:B) for INC (incorporated), SA (surface-applied), and SA-NR (surface-applied/no new residue) treatments from 0-5 cm (a) and 5-10 cm (b). Fungal:bacterial ratios are calculated by dividing total residue-derived fungal biomass (ng PLFA-C/g soil) by the total residue-derived bacterial biomass (ng PLFA-C g^{-1} soil). Panels correspond to soil core harvest times (i.e., 6, 12, and 30 months post establishment of the experiment). Data represent averages and standard errors (n=4).

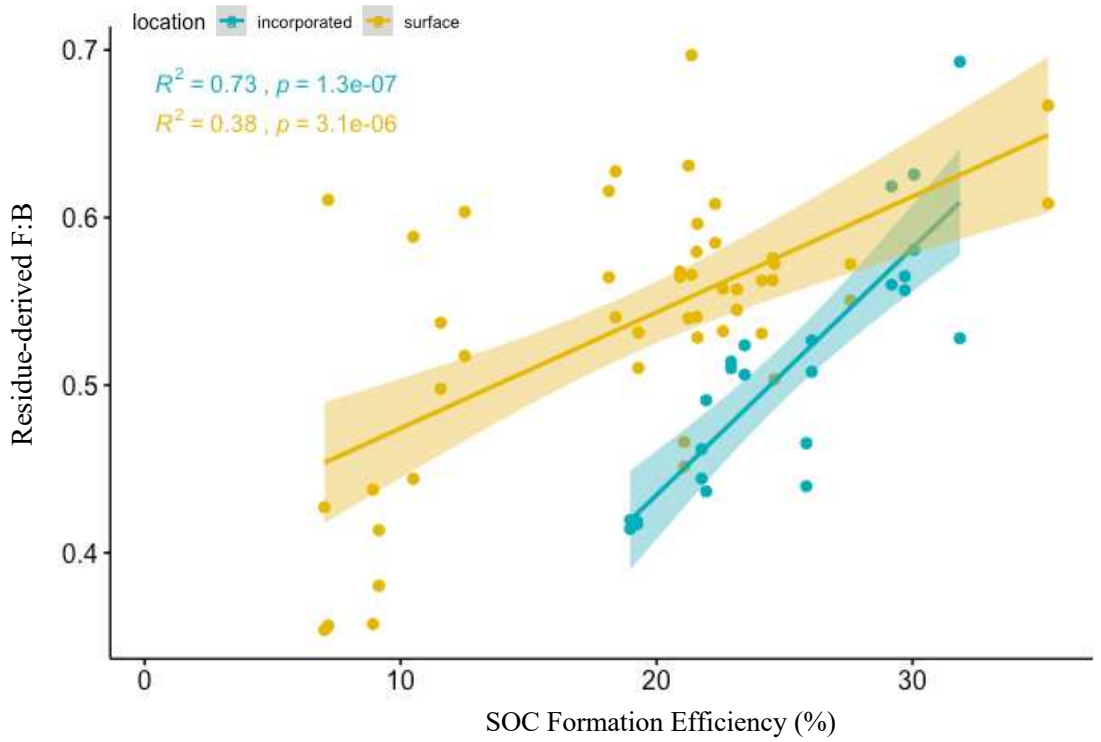

Figure 9. Correlation between residue-derived fungal C:residue-derived bacterial C ratios (F:B) and soil organic carbon (SOC) formation efficiency (%) from 0-10 cm for incorporated (INC) and surface-applied (SA and SA-NR) residue treatments at all timepoints (n=24 for incorporated; n=48 for surface-applied).

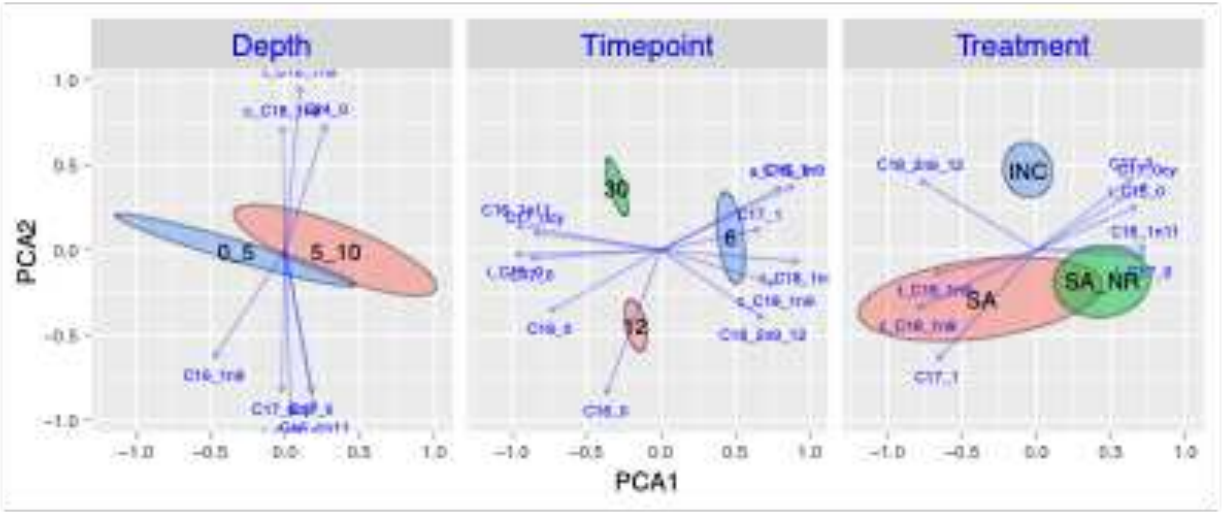

Figure 10. Principle component analysis (PCA) of enriched microbial biomass (ng PLFA-C g^{-1} soil) from 0-10 cm. Panels correspond to factors (i.e., depth, timepoint, and treatment). 0_5 and 5_10 correspond to 0-5 cm and 5-10 cm, respectively. 6, 12, and 30 correspond to soil core harvest times (i.e., 6, 12, and 30 months post establishment of experiment, respectively). INC, SA, and SA_NR correspond to residue treatments, (i.e., incorporated, surface-applied, and surface-applied /no new residue, respectively).

CHAPTER 4: DISCUSSION

Our study indicated significant treatment differences in the residue-derived C dynamics of our system. Most interestingly, our incorporated treatment (INC) accrued two to three times as much residue-derived SOC, lost twice as much residue C as CO_2 and recovered approximately half of the amount of residue C as residue than did surface-applied treatments after 6 months (Table 2). This data suggests that SOC is initially forming more rapidly and, according to our SOC formation efficiency calculations (Figure 4), more efficiently upon incorporation of residue. After 30 months, however, differences between treatments converged, corroborating results found by Mitchell et al. (2018). While INC still accrued more residue-derived SOC and retained far less residue C as residue, INC apparently lost less residue C as CO_2 than SA and SA-NR after 30 months. Furthermore, regardless of residue placement location, the efficiency of SOC formation was approximately 23% after 30 months, suggesting that the surface application of residue resulted in more efficient SOC formation in later stages of the experiment. These differing temporal dynamics in C movement and SOC formation efficiency between treatments indicate that residue placement alters the dynamics of the pathways of SOC formation.

Approximately 30-60% of residue C initially added was not recovered across treatment and timepoint (Table 2). This may be a consequence of our soil sampling method. Specifically, residue C was initially distributed within the collar, which had a diameter of 10 cm. Upon soil core extraction, however, soil cores were taken for 10-100 cm depths with a Gidding's rig that had a 6.25 cm diameter coring tube. Therefore, any residue C that may have moved down the soil profile in between the 6.25 cm diameter of the coring tube and 10 cm diameter of the collar would not be recovered. This may also explain why surface-applied residue C recovery was

generally greater than that of INC. Particularly, because residue C was incorporated throughout 0-10 cm of INC, the movement of that residue C as SOC or residue into the unrecovered soil from 10-100 cm was more likely than for residue applied on the surface. Although we were not able to recover all of the residue C initially applied, the residue C that we did recover helps to elucidate the different mechanisms responsible for SOM formation in our system.

Residue-derived organic C content in bulk soil had a linear relationship with mean weight diameter (MWD) in incorporated treatments (r^2=.34, p=.0029), in comparison to no relationship in surface applied treatments (r^2=.03, p=.21) (Figure 6). Because only INC had residue incorporated within the soil profile, it is likely that the macroaggregates in INC contained far more residue than did SA or SA-NR, as OC serves as a nucleus for aggregate formation (Golchin et al., 1994). Thus, any events that trigger aggregate disruption have the potential to expose far more residue C to microbial decomposition (Elliott & Coleman, 1988; Balesdent et al., 2000) or leaching in INC, compared to SA or SA-NR. For example, frequent wet-dry cycles, such as those caused by the regular irrigation events seen in our system, can cause macroaggregate disruption and thus allow for frequent microbial access to substrate (Adu & Oades, 1978; Gillabel et al., 2007; Schimel et al., 2011). These cycles may be even more intense in incorporated residue treatments due to a greater susceptibility to evaporation (Balesdent et al., 2000).

However, residue-derived CO_2 respiration indicates that residue C lost as CO_2 was actually greater in SA and SA-NR during regular irrigation in the growing season (Figure 2). This suggests that wet-dry cycles did not cause aggregate disruption and, thus, microbial decomposition of unprotected residue C in INC. Rather, this supports findings by Denef et al. (2001), which indicate that wet-dry cycles actually promote aggregate stabilization, rather than disruption. Additionally, irrigation water provides a rich source of calcium ions that, when

combined with the high levels of carbonate in our system, can stabilize aggregates (Baldock & Skjemstad, 2000; Six et al., 2004). Considering that all treatments seemed to have greater MWD's after periods of irrigation (Figure 5), the seasonal dynamics of MWD's in our study may further confirm the stabilizing effect of dry-wet cycles upon aggregates. Increased water availability is believed to bridge the spatial gap between microbes and residue, enabling increased microbial decomposition (Or et al., 2007). Thus, increased microbial access to residue during periods of irrigation coupled with heightened microbial activity during the growing season due to root exudates, may provide more microbially-derived binding agents for macroaggregate formation, hence the larger MWD's at baseline and 12 months.

The incorporation of residue stimulates a larger pool of actively-decomposing microbes than does the surface-application of residue (Holland & Coleman; 1987). This is confirmed by the greater residue-derived microbial biomass (Figure 7) and residue-derived CO_2 respired (Table 2) seen in INC after 6 months. With greater microbial decomposition and more microbially-derived binding agents available for macroaggregate formation (Six et al., 2004; Denef & Six, 2005), INC demonstrated larger MWD's at 6 months than SA and SA-NR (Figure 5). Because this study was conducted in a plot that was historically under NT management, fresh residue inputs to the 5-10 cm depth were likely novel and, thus, provided greater potential for increased aggregation at depth. At 12 months, the MWD's of INC and SA-NR were both greater than that of SA, albeit this was only significant from 5-10 cm (Figure 5). This parallel between INC and SA-NR may suggest that physical disturbance has an effect upon aggregation even a year after disturbance, particularly at depth.

Ultimately, our data suggests that the protection of residue C from further decomposition heavily depends upon occlusion within macroaggregates when residue is incorporated. In

contrast, protection of surface applied residue seemed to be unrelated to aggregation, as seen by the lack of relationship between residue-derived organic C and MWD (Figure 6). This is further validated by our correlations of SOC formation efficiencies with enriched F:B. SOC formation efficiency was found to be much more highly correlated with enriched F:B ratios in incorporated residue treatments (r^2=.73) than in surface applied residue treatments (r^2=.38) (Figure 9). Because macroaggregate formation is greatly induced by fungal activity (Six et al., 1998; Denef et al., 2001), the greater association of SOC formation efficiency with fungal activity in INC may indicate a greater dependence upon macroaggregates for residue C protection. In contrast, surface-applied systems may rely more greatly on protection within more resilient microaggregates or through mineral-binding. The varying mechanisms responsible for residue C protection from microbial decomposition are of great importance, as microbial access to residue limits SOC formation (Schmidt et al., 2011; Lehmann & Kleber, 2015; Waring et al., 2020).

Soil microbial communities are highly dynamic, with turnover times estimated to be 2-3 weeks (Fisk et al., 1998; Lipson et al., 2001). Therefore, PLFA's give us a snapshot of the microbial community and do not allow us to visualize changes in community between soil core harvest times (Schmidt et al., 2007). Residue-derived F:B ranged from approximately 0.4 to 0.6 in our study (Figure 8), as did total F:B (data not included). These values seem to be higher than those previously reported at our research location (Stewart et al., 2018). This may be an effect of the NT legacy of our research plot, as NT reportedly leads to higher F:B (Beare et al., 1992; Frey et al., 1999). Additionally, one of the PLFA biomarkers that we used as an indicator of AMF (16:1ω5) can also serve as an indicator for gram-negative bacteria (Nichols et al., 1986). Based on preliminary analysis of our neutral-lipid fatty acid (NLFA) data, 16:1ω5 was largely representative of AMF in our study, hence we concluded that it is appropriate to use 16:1ω5 as

an indicator of AMF. However, this may have led to an overestimation of fungal compared to bacterial biomass and, thus, greater F:B. Nonetheless, because these potential discrepancies affect all of our treatments equally, they should not affect our analysis between treatments.

Consistent with several studies that found no difference in F:B between NT and CT (reviewed by Strickland and Rousk, 2010; Chen et al., 2020), our PLFA analysis indicated that there was no significant difference in residue-derived F:B between treatments (Figure 8). This may be related to the lack of moisture limitation in our study due to irrigation. Specifically, Frey et al. (1999) found that the effect of tillage treatment on F:B was not significant when adjusting for differences in soil moisture. However, our data simultaneously revealed that INC had over twice the amount of residue-derived microbial biomass as SA and SA-NR throughout the first year of the study (Figure 7). This indicates that, despite residue-derived F:B's being similar, INC had much more residue-derived fungal biomass than did SA and SA-NR. The higher levels of residue-derived fungal biomass and greater MWD's in INC are consistent with the role that fungi play in stabilizing macroaggregates (Six et al.,1998; Denef et al., 2001).

Although our study demonstrates a specific linkage between fungi and residue incorporation, this does not invalidate the importance of fungi for SOC formation and protection in surface-applied residue treatments. Fungi are reported to play a critical role in C decomposition and stabilization (Beare et al., 1992; Beare et al., 1997; Malik et al., 2016; Chen et al., 2020) and, by further examining the fungal community, we can better elucidate these fungal roles. Using PLFA-C, we were able to highlight the contributions of different members of the fungal community to our observed residue C dynamics. Over a period of 30 months, our study confirmed a fungal shift from a residue-derived saprotrophic to arbuscular mycorrhizal fungi (AMF) presence among all treatments (Figure 10). It is believed that saprotrophs possess

physiological traits that enable them to break down structural OM directly (Herman et al., 2012). In contrast, AMF lack these characteristics and depend on the saprotrophic release of degraded organic substrate in order to provide nutrients to their plant host (reviewed by Van Der Heijden et al., (2008); Smith & Read, 2008; Herman et al., 2012). Therefore, saprotrophs have often been identified with the earlier stages of decomposition, in contrast to AMF (Denef et al., 2007).

Our data further indicated that differences in residue-derived microbial community based on residue location placement were heavily influenced by several specific biomarkers (Figure 10). Of note were two saprotrophic biomarkers: 18:2ω6 was largely associated with INC and cis-18:1ω7 was strongly related to SA. This suggests that specific species of saprotrophs may play differing roles in SOC formation, potentially due to different preferences or abilities to degrade varying substrate qualities. Knowledge on saprotrophs is fairly limited to date; thus, more research in this field is warranted.

Interestingly, the significant residue-derived microbial biomarkers of undisturbed treatments paralleled those of early microbial communities, while residue-derived microbial biomarkers of disturbed treatments corresponded to those of later microbial communities (Figure 10). Recent work highlights two highly efficient pathways of SOC formation: a dissolved organic carbon (DOC)-microbial pathway, by which non-structural compounds are leached and microbially incorporated during initial stages of decomposition, and a physical transfer pathway, by which more structural components are physically transferred into the mineral soil during later stages of decomposition (Cotrufo et al., 2015). SOC formed through the DOC-microbial pathway is believed to be stabilized by association with minerals, while SOC formed via the physical transfer pathway can be stabilized by aggregate occlusion. These temporally separated formation pathways are largely dependent upon a linear shift in residue chemistry over time (Poll et al.,

2008; reviewed by Strickland & Rousk, 2010; Cotrufo et al., 2015). The parallel between residue-derived microbial communities across time and between treatments may suggest that substrate quality availability is driving the composition of the residue-derived community in our system and, hence, SOC formation.

In particular, the surface-application of residue follows the linear shift in the dynamics of SOC formation pathways, characterized by an initial DOC-microbial pathway, later followed by a physical transfer pathway. The DOC-microbial pathway likely peaked at the beginning of irrigation just after 6 months, explaining the low SOC formation efficiency up until 6 months and the jump in SOC formation efficiency at 12 months (Figure 4). This additionally explains the lack of correlation between MWD and residue-derived soil organic C (Figure 6), as residue-derived organic C is accumulating through microbial assimilation of DOM or sorption of DOM to minerals, rather than through aggregation. After 12 months, SOC formation shifts to the physical-transfer pathway, which is confirmed by the consistently high SOC formation efficiency (Figure 4), the decrease in residue-derived microbial biomass (Figure 7), and the further accumulation in residue-derived organic C (Table 2).

In contrast, the incorporation of residue distributes labile and structural compounds into the soil matrix, allowing for the DOM-microbial and the physical transfer pathways to occur simultaneously. This is supported by the high SOC formation efficiencies seen in INC throughout the first 12 months (Figure 4), which likely peaks in between 6 and 12 months due to added DOC from irrigation. Furthermore, the high initial microbial biomass (Figure 7), the strong relationship between MWD and residue-derived C (Figure 6), and the fast residue mass loss (Figure 3) all testify for the occurrence of both SOC formation pathways concurrently. As

labile substrates become limited and residue C becomes protected within aggregates, SOC formation efficiencies in INC drop (Figure 4) and SOC formation (Table 2) stagnates.

CHAPTER 5: CONCLUSION

To elucidate our understanding of tillage, we used isotopically-labeled residue to track the dynamics of incorporated vs. surface-applied residue-derived C over a period of 30 months. Our study indicated that the incorporation of residue in a semi-arid, irrigated system promoted more efficient SOC formation and greater C accrual in the short-term. However, after 30 months, there were no differences in SOM formation efficiency depending on residue placement, with only modestly greater C accrual in INC versus SA. Our study suggests that these differences were due to differences in timing of SOC formation pathways and the mechanisms by which residue C was protected from microbial decomposition. Particularly, SOC formation pathways occurred simultaneously in the incorporated residue treatment, while surface-applied residue treatments experienced a linear shift from one SOC formation to the next. Furthermore, the incorporated residue treatment depended on physical protection through macroaggregates for residue protection, while surface-applied residue treatments may have depended more greatly on other mechanisms for protection, such as microaggregates and mineral-binding. These data indicate that aggregation can play a critical role in SOC formation in agroecosystems and should be included in models assessing C accrual. In order to understand the effects of aggregates, microbes, residue placement location, and disturbance on long-term C stabilization, it would be highly informative to analyze the distribution of mineral-associated organic matter (MAOM) and particulate organic matter (POM) within aggregates.

REFERENCES

Adu, J. K., & Oades, J. M. (1978). Physical factors influencing decomposition of organic materials in soil aggregates. *Soil Biology and Biochemistry*, *10*(2). https://doi.org/10.1016/0038-0717(78)90080-9

Angers, D. A., Bolinder, M. A., Carter, M. R., Gregorich, E. G., Drury, C. F., Liang, B. C., Voroney, R. P., Simard, R. R., Donald, R. G., Beyaert, R. P., & Martel, J. (1997). Impact of tillage practices on organic carbon and nitrogen storage in cool, humid soils of eastern Canada. *Soil and Tillage Research*, *41*(3–4). https://doi.org/10.1016/S0167-1987(96)01100-2

Baker, J. M., Ochsner, T. E., Venterea, R. T., & Griffis, T. J. (2007). Tillage and soil carbon sequestration—What do we really know? *Agriculture, Ecosystems & Environment*, *118*(1–4). https://doi.org/10.1016/j.agee.2006.05.014

Baldock, J. A., & Skjemstad, J. O. (2000). Role of the soil matrix and minerals in protecting natural organic materials against biological attack. *Organic Geochemistry*, *31*(7–8). https://doi.org/10.1016/S0146-6380(00)00049-8

Balesdent, J., Chenu, C., & Balabane, M. (2000). Relationship of soil organic matter dynamics to physical protection and tillage. *Soil and Tillage Research*, *53*(3–4). https://doi.org/10.1016/S0167-1987(99)00107-5

Bayer, C., Martin-Neto, L., Mielniczuk, J., Pavinato, A., & Dieckow, J. (2006). Carbon sequestration in two Brazilian Cerrado soils under no-till. *Soil and Tillage Research*, *86*(2). https://doi.org/10.1016/j.still.2005.02.023

Beare, M. H., Hu, S., Coleman, D. C., & Hendrix, P. F. (1997). Influences of mycelial fungi on soil aggregation and organic matter storage in conventional and no-tillage soils. *Applied Soil Ecology*, *5*(3). https://doi.org/10.1016/S0929-1393(96)00142-4

Beare, M. H., Parmelee, R. W., Hendrix, P. F., Cheng, W., Coleman, D. C., & Crossley, D. A. (1992). Microbial and Faunal Interactions and Effects on Litter Nitrogen and Decomposition in Agroecosystems. *Ecological Monographs*, *62*(4). https://doi.org/10.2307/2937317

Blake, G. R. (2015). *Bulk Density*. https://doi.org/10.2134/agronmonogr9.1.c30

Blanco-Canqui, H., & Lal, R. (2008). No-Tillage and Soil-Profile Carbon Sequestration: An On-Farm Assessment. *Soil Science Society of America Journal*, *72*(3). https://doi.org/10.2136/sssaj2007.0233

Boer, W. de, Folman, L. B., Summerbell, R. C., & Boddy, L. (2005). Living in a fungal world: impact of fungi on soil bacterial niche development. *FEMS Microbiology Reviews*, *29*(4). https://doi.org/10.1016/j.femsre.2004.11.005

Bossio, D. A., & Scow, K. M. (1995). Impact of carbon and flooding on the metabolic diversity of microbial communities in soils. *Applied and Environmental Microbiology*, *61*(11). https://doi.org/10.1128/aem.61.11.4043-4050.1995

Bossuyt, H., Denef, K., Six, J., Frey, S. D., Merckx, R., & Paustian, K. (2001). Influence of microbial populations and residue quality on aggregate stability. *Applied Soil Ecology*, *16*(3). https://doi.org/10.1016/S0929-1393(00)00116-5

Buyanovsky, G. A., Aslam, M., & Wagner, G. H. (1994). Carbon Turnover in Soil Physical Fractions. *Soil Science Society of America Journal*, *58*(4). https://doi.org/10.2136/sssaj1994.03615995005800040023x

Cambardella, C. A., & Elliott, E. T. (1992). Particulate Soil Organic-Matter Changes across a Grassland Cultivation Sequence. *Soil Science Society of America Journal*, *56*(3). https://doi.org/10.2136/sssaj1992.03615995005600030017x

Carney, K. M., Hungate, B. A., Drake, B. G., & Megonigal, J. P. (2007). Altered soil microbial community at elevated CO2 leads to loss of soil carbon. *Proceedings of the National Academy of Sciences*, *104*(12). https://doi.org/10.1073/pnas.0610045104

Chen, H., Dai, Z., Veach, A. M., Zheng, J., Xu, J., & Schadt, C. W. (2020). Global meta-analyses show that conservation tillage practices promote soil fungal and bacterial biomass. *Agriculture, Ecosystems & Environment*, *293*. https://doi.org/10.1016/j.agee.2020.106841

Cotrufo, M. F., Soong, J. L., Horton, A. J., Campbell, E. E., Haddix, M. L., Wall, D. H., & Parton, W. J. (2015). Formation of soil organic matter via biochemical and physical pathways of litter mass loss. *Nature Geoscience*, *8*(10). https://doi.org/10.1038/ngeo2520

de Gryze, S., Six, J., & Merckx, R. (2006). Quantifying water-stable soil aggregate turnover and its implication for soil organic matter dynamics in a model study. *European Journal of Soil Science*, *57*(5). https://doi.org/10.1111/j.1365-2389.2005.00760.x

Denef, K., Bubenheim, H., Lenhart, K., Vermeulen, J., van Cleemput, O., Boeckx, P., & Müller, C. (2007). Community shifts and carbon translocation within metabolically-active rhizosphere microorganisms in grasslands under elevated CO₂ *Biogeosciences*, *4*(5). https://doi.org/10.5194/bg-4-769-2007

Denef, K., & Six, J. (2005). Clay mineralogy determines the importance of biological versus abiotic processes for macroaggregate formation and stabilization. *European Journal of Soil Science*, *56*(4). https://doi.org/10.1111/j.1365-2389.2004.00682.x

Denef, K., Six, J., Bossuyt, H., Frey, S. D., Elliott, E. T., Merckx, R., & Paustian, K. (2001). Influence of dry–wet cycles on the interrelationship between aggregate, particulate organic matter, and microbial community dynamics. *Soil Biology and Biochemistry*, *33*(12–13). https://doi.org/10.1016/S0038-0717(01)00076-1

Elliott, E. T., & Coleman, D. C. (1988). Let the Soil Work for Us. *Ecological Bulletins*, *39*, 23–32. http://www.jstor.org/stable/20112982

Fisk, M. C., Schmidt, S. K., & Seastedt, T. R. (1998). Topographic Patterns of above- and Belowground Production and Nitrogen Cycling in Alpine Tundra. *Ecology*, *79*(7). https://doi.org/10.2307/176820

Frey, S. D., Elliott, E. T., & Paustian, K. (1999). Bacterial and fungal abundance and biomass in conventional and no-tillage agroecosystems along two climatic gradients. *Soil Biology and Biochemistry*, *31*(4). https://doi.org/10.1016/S0038-0717(98)00161-8

Frostegård, A., & Bååth, E. (1996). The use of phospholipid fatty acid analysis to estimate bacterial and fungal biomass in soil. *Biology and Fertility of Soils*, *22*(1–2). https://doi.org/10.1007/BF00384433

Gillabel, J., Denef, K., Brenner, J., Merckx, R., & Paustian, K. (2007). Carbon Sequestration and Soil Aggregation in Center-Pivot Irrigated and Dryland Cultivated Farming Systems. *Soil Science Society of America Journal*, *71*(3). https://doi.org/10.2136/sssaj2006.0215

Golchin, A., Oades, J., Skjemstad, J., & Clarke, P. (1994). Soil structure and carbon cycling. *Soil Research*, *32*(5). https://doi.org/10.1071/SR9941043

Haddix, M. L., Gregorich, E. G., Helgason, B. L., Janzen, H., Ellert, B. H., & Francesca Cotrufo, M. (2020). Climate, carbon content, and soil texture control the independent formation and

persistence of particulate and mineral-associated organic matter in soil. *Geoderma*, *363*. https://doi.org/10.1016/j.geoderma.2019.114160

Haddix, M. L., Paul, E. A., & Cotrufo, M. F. (2016). Dual, differential isotope labeling shows the preferential movement of labile plant constituents into mineral-bonded soil organic matter. *Global Change Biology*, *22*(6). https://doi.org/10.1111/gcb.13237

Halvorson, A. D., & Stewart, C. E. (2015). Stover Removal Affects No-Till Irrigated Corn Yields, Soil Carbon, and Nitrogen. *Agronomy Journal*, *107*(4). https://doi.org/10.2134/agronj15.0074

Havlin, J. L., Kissel, D. E., Maddux, L. D., Claassen, M. M., & Long, J. H. (1990). Crop Rotation and Tillage Effects on Soil Organic Carbon and Nitrogen. *Soil Science Society of America Journal*, *54*(2). https://doi.org/10.2136/sssaj1990.03615995005400020026x

Hendrix, P. F., Parmelee, R. W., Crossley, , D. A., Coleman, D. C., Odum, E. P., & Groffman, P. M. (1986). Detritus Food Webs in Conventional and No-Tillage Agroecosystems. *BioScience*, *36*(6). https://doi.org/10.2307/1310259

Herman, D. J., Firestone, M. K., Nuccio, E., & Hodge, A. (2012). Interactions between an arbuscular mycorrhizal fungus and a soil microbial community mediating litter decomposition. *FEMS Microbiology Ecology*, *80*(1). https://doi.org/10.1111/j.1574-6941.2011.01292.x

Holland, E. A., & Coleman, D. C. (1987). Litter Placement Effects on Microbial and Organic Matter Dynamics in an Agroecosystem. *Ecology*, *68*(2). https://doi.org/10.2307/1939274

Jastrow, J. D., Amonette, J. E., & Bailey, V. L. (2007). Mechanisms controlling soil carbon turnover and their potential application for enhancing carbon sequestration. *Climatic Change*, *80*(1–2). https://doi.org/10.1007/s10584-006-9178-3

Kleber, M., Eusterhues, K., Keiluweit, M., Mikutta, C., Mikutta, R., & Nico, P. S. (2015). *Mineral–Organic Associations: Formation, Properties, and Relevance in Soil Environments*. https://doi.org/10.1016/bs.agron.2014.10.005

Kögel-Knabner, I., Guggenberger, G., Kleber, M., Kandeler, E., Kalbitz, K., Scheu, S., Eusterhues, K., & Leinweber, P. (2008). Organo-mineral associations in temperate soils: Integrating biology, mineralogy, and organic matter chemistry. *Journal of Plant Nutrition and Soil Science*, *171*(1). https://doi.org/10.1002/jpln.200700048

Kong, A. Y. Y., Scow, K. M., Córdova-Kreylos, A. L., Holmes, W. E., & Six, J. (2011). Microbial community composition and carbon cycling within soil microenvironments of conventional, low-input, and organic cropping systems. *Soil Biology and Biochemistry*, *43*(1). https://doi.org/10.1016/j.soilbio.2010.09.005

Lal, R., Negassa, W., & Lorenz, K. (2015). Carbon sequestration in soil. *Current Opinion in Environmental Sustainability*, *15*. https://doi.org/10.1016/j.cosust.2015.09.002

Lehmann, J., & Kleber, M. (2015). The contentious nature of soil organic matter. *Nature*, *528*(7580). https://doi.org/10.1038/nature16069

Leichty, S., Cotrufo, M. F., & Stewart, C. E. (2020). Less efficient residue-derived soil organic carbon formation under no-till irrigated corn. *Soil Science Society of America Journal*, *84*(6). https://doi.org/10.1002/saj2.20136

Lipson, D. A., Raab, T. K., Schmidt, S. K., & Monson, R. K. (2001). An empirical model of amino acid transformations in an alpine soil. *Soil Biology and Biochemistry*, *33*(2). https://doi.org/10.1016/S0038-0717(00)00128-0

Malik, A. A., Chowdhury, S., Schlager, V., Oliver, A., Puissant, J., Vazquez, P. G. M., Jehmlich, N., von Bergen, M., Griffiths, R. I., & Gleixner, G. (2016). Soil Fungal:Bacterial Ratios Are

Linked to Altered Carbon Cycling. *Frontiers in Microbiology*, *7*. https://doi.org/10.3389/fmicb.2016.01247

Manley, J., van Kooten, G. C., Moeltner, K., & Johnson, D. W. (2005). Creating Carbon Offsets in Agriculture through No-Till Cultivation: A Meta-Analysis of Costs and Carbon Benefits. *Climatic Change*, *68*(1–2). https://doi.org/10.1007/s10584-005-6010-4

Mitchell, E., Scheer, C., Rowlings, D., Conant, R. T., Cotrufo, M. F., & Grace, P. (2018). Amount and incorporation of plant residue inputs modify residue stabilisation dynamics in soil organic matter fractions. *Agriculture, Ecosystems & Environment*, *256*. https://doi.org/10.1016/j.agee.2017.12.006

Nichols, P., Stulp, B. K., Jones, J. G., & White, D. C. (1986). Comparison of fatty acid content and DNA homology of the filamentous gliding bacteriaVitreoscilla, Flexibacter, Filibacter. *Archives of Microbiology*, *146*(1). https://doi.org/10.1007/BF00690149

Or, D., Smets, B. F., Wraith, J. M., Dechesne, A., & Friedman, S. P. (2007). Physical constraints affecting bacterial habitats and activity in unsaturated porous media – a review. *Advances in Water Resources*, *30*(6–7). https://doi.org/10.1016/j.advwatres.2006.05.025

Paul, E. (2014). *Soil Microbiology, Ecology and Biochemistry*. 0–598.

Paustian, K., Andrén, O., Janzen, H. H., Lal, R., Smith, P., Tian, G., Tiessen, H., Noordwijk, M., & Woomer, P. L. (1997). Agricultural soils as a sink to mitigate CO2 emissions. *Soil Use and Management*, *13*(s4). https://doi.org/10.1111/j.1475-2743.1997.tb00594.x

Paustian, K., Lehmann, J., Ogle, S., Reay, D., Robertson, G. P., & Smith, P. (2016). Climate-smart soils. *Nature*, *532*(7597). https://doi.org/10.1038/nature17174

Poll, C., Marhan, S., Ingwersen, J., & Kandeler, E. (2008). Dynamics of litter carbon turnover and microbial abundance in a rye detritusphere. *Soil Biology and Biochemistry*, *40*(6). https://doi.org/10.1016/j.soilbio.2007.04.002

Sanderman, J., Hengl, T., & Fiske, G. J. (2017). Soil carbon debt of 12,000 years of human land use. *Proceedings of the National Academy of Sciences*, *114*(36). https://doi.org/10.1073/pnas.1706103114

Schimel, J. P., Wetterstedt, J. Å. M., Holden, P. A., & Trumbore, S. E. (2011). Drying/rewetting cycles mobilize old C from deep soils from a California annual grassland. *Soil Biology and Biochemistry*, *43*(5). https://doi.org/10.1016/j.soilbio.2011.01.008

Schmidt, M. W. I., Torn, M. S., Abiven, S., Dittmar, T., Guggenberger, G., Janssens, I. A., Kleber, M., Kögel-Knabner, I., Lehmann, J., Manning, D. A. C., Nannipieri, P., Rasse, D. P., Weiner, S., & Trumbore, S. E. (2011). Persistence of soil organic matter as an ecosystem property. *Nature*, *478*(7367). https://doi.org/10.1038/nature10386

Schmidt, S. K., Costello, E. K., Nemergut, D. R., Cleveland, C. C., Reed, S. C., Weintraub, M. N., Meyer, A. F., & Martin, A. M. (2007). BIOGEOCHEMICAL CONSEQUENCES OF RAPID MICROBIAL TURNOVER AND SEASONAL SUCCESSION IN SOIL. *Ecology*, *88*(6). https://doi.org/10.1890/06-0164

Shukla, P.R., Skea, J., Calvo Buendia, E., Masson-Delmotte, V., Pörtner, H.-O., Roberts, D.C., Zhai, P., Slade, R., Connors, S., van Diemen, R., Ferrat, M., Haughey, E., Luz, S., Neogi, S., Pathak, M., Petzold, J., Portugal Pereira, J., Vyas, P., Huntley, E., Kissick, K., Belkacemi, M., Malley, J., etc. (2019). Climate Change and Land: an IPCC special report on climate change, desertification, land degradation, sustainable land management, food security, and greenhouse gas fluxes in terrestrial ecosystems. In Press.

Six, J., Bossuyt, H., Degryze, S., & Denef, K. (2004). A history of research on the link between (micro)aggregates, soil biota, and soil organic matter dynamics. *Soil and Tillage Research*, *79*(1). https://doi.org/10.1016/j.still.2004.03.008

Six, J., Conant, R. T., Paul, E. A., & Paustian, K. (2002). Stabilization mechanisms of soil organic matter: Implications for C-saturation of soils. *Plant and Soil*, *241*(2). https://doi.org/10.1023/A:1016125726789

Six, J., Elliott, E. T., Paustian, K., & Doran, J. W. (1998). Aggregation and Soil Organic Matter Accumulation in Cultivated and Native Grassland Soils. *Soil Science Society of America Journal*, *62*(5). https://doi.org/10.2136/sssaj1998.03615995006200050032x

Six, J., Frey, S. D., Thiet, R. K., & Batten, K. M. (2006). Bacterial and Fungal Contributions to Carbon Sequestration in Agroecosystems. *Soil Science Society of America Journal*, *70*(2). https://doi.org/10.2136/sssaj2004.0347

Six, J., & Paustian, K. (2014). Aggregate-associated soil organic matter as an ecosystem property and a measurement tool. *Soil Biology and Biochemistry*, *68*. https://doi.org/10.1016/j.soilbio.2013.06.014

SMITH, PETE., POWLSON, D. S., GLENDINING, M. J., & SMITH, JO. U. (1998). Preliminary estimates of the potential for carbon mitigation in European soils through no-till farming. *Global Change Biology*, *4*(6). https://doi.org/10.1046/j.1365-2486.1998.00185.x

Smith, S., & Read, D. (2008). *Mycorrhizal Symbiosis* (3rd ed.).

Sokol, N. W., Sanderman, J., & Bradford, M. A. (2019). Pathways of mineral-associated soil organic matter formation: Integrating the role of plant carbon source, chemistry, and point of entry. *Global Change Biology*, *25*(1). https://doi.org/10.1111/gcb.14482

Stewart, C. E., Roosendaal, D. L., Manter, D. K., Delgado, J. A., & del Grosso, S. (2018). Interactions of Stover and Nitrogen Management on Soil Microbial Community and Labile Carbon under Irrigated No-Till Corn. *Soil Science Society of America Journal*, *82*(2). https://doi.org/10.2136/sssaj2017.07.0229

Stockmann, U., Adams, M. A., Crawford, J. W., Field, D. J., Henakaarchchi, N., Jenkins, M., Minasny, B., McBratney, A. B., Courcelles, V. de R. de, Singh, K., Wheeler, I., Abbott, L., Angers, D. A., Baldock, J., Bird, M., Brookes, P. C., Chenu, C., Jastrow, J. D., Lal, R., … Zimmermann, M. (2013). The knowns, known unknowns and unknowns of sequestration of soil organic carbon. *Agriculture, Ecosystems & Environment*, *164*. https://doi.org/10.1016/j.agee.2012.10.001

Strickland, M. S., & Rousk, J. (2010). Considering fungal:bacterial dominance in soils – Methods, controls, and ecosystem implications. *Soil Biology and Biochemistry*, *42*(9). https://doi.org/10.1016/j.soilbio.2010.05.007

TISDALL, J. M., & OADES, J. M. (1982). Organic matter and water-stable aggregates in soils. *Journal of Soil Science*, *33*(2). https://doi.org/10.1111/j.1365-2389.1982.tb01755.x

Trivedi, P., Rochester, I. J., Trivedi, C., van Nostrand, J. D., Zhou, J., Karunaratne, S., Anderson, I. C., & Singh, B. K. (2015). Soil aggregate size mediates the impacts of cropping regimes on soil carbon and microbial communities. *Soil Biology and Biochemistry*, *91*. https://doi.org/10.1016/j.soilbio.2015.08.034

USDA National Agricultural Statistics Service (2017). Census of Agriculture. Complete data available at www.nass.usda.gov/AgCensus

van der Heijden, M. G. A., Bardgett, R. D., & van Straalen, N. M. (2008). The unseen majority: soil microbes as drivers of plant diversity and productivity in terrestrial ecosystems. *Ecology Letters*, *11*(3). https://doi.org/10.1111/j.1461-0248.2007.01139.x

van Groenigen, K.-J., Bloem, J., Bååth, E., Boeckx, P., Rousk, J., Bodé, S., Forristal, D., & Jones, M. B. (2010). Abundance, production and stabilization of microbial biomass under conventional and reduced tillage. *Soil Biology and Biochemistry*, *42*(1). https://doi.org/10.1016/j.soilbio.2009.09.023

VandenBygaart, A. J., Gregorich, E. G., & Angers, D. A. (2003). Influence of agricultural management on soil organic carbon: A compendium and assessment of Canadian studies. *Canadian Journal of Soil Science*, *83*(4). https://doi.org/10.4141/S03-009

Waring, B. G., Sulman, B. N., Reed, S., Smith, A. P., Averill, C., Creamer, C. A., Cusack, D. F., Hall, S. J., Jastrow, J. D., Jilling, A., Kemner, K. M., Kleber, M., Liu, X. A., Pett-Ridge, J., & Schulz, M. (2020). From pools to flow: The PROMISE framework for new insights on soil carbon cycling in a changing world. *Global Change Biology*, *26*(12). https://doi.org/10.1111/gcb.15365